

## Electron spin resonance studies of $\text{Co}(\text{tbp})\cdot\text{C}_{60}$ single crystal

This article has been downloaded from IOPscience. Please scroll down to see the full text article.

2002 J. Phys.: Condens. Matter 14 3993

(<http://iopscience.iop.org/0953-8984/14/15/313>)

View [the table of contents for this issue](#), or go to the [journal homepage](#) for more

Download details:

IP Address: 171.66.16.104

The article was downloaded on 18/05/2010 at 06:28

Please note that [terms and conditions apply](#).

## Electron spin resonance studies of Co(tbp)·C<sub>60</sub> single crystal

H Tanaka<sup>1</sup>, K Marumoto<sup>1</sup>, S Kuroda<sup>1</sup>, T Ishii<sup>2</sup>, R Kanehama<sup>2</sup>,  
N Aizawa<sup>2</sup>, H Matsuzaka<sup>2</sup>, K Sugiura<sup>2</sup>, H Miyasaka<sup>2</sup>, T Kodama<sup>2</sup>,  
K Kikuchi<sup>2</sup>, I Ikemoto<sup>2</sup> and M Yamashita<sup>2</sup>

<sup>1</sup> Department of Applied Physics, Nagoya University, Nagoya, 464-8603, Japan

<sup>2</sup> Department of Chemistry, Tokyo Metropolitan University, Minamiosawa1-1,  
Hachioji 192-0397, Japan

E-mail: h002304d@mbox.media.nagoya-u.ac.jp (H Tanaka)

Received 5 February 2002

Published 4 April 2002

Online at [stacks.iop.org/JPhysCM/14/3993](http://stacks.iop.org/JPhysCM/14/3993)

### Abstract

ESR measurements have been made on a newly synthesized cocrystallite of C<sub>60</sub> with the Co<sup>II</sup> complex of 5, 10, 15, 20-tetrakis[3, 5-(di-*tert*-butyl)phenyl]porphyrin (tbp) single crystal to study the strong intermolecular interactions which are suggested by x-ray structural analyses. A single anisotropic ESR absorption line is observed at room temperature with the principal  $g$ -values  $g_{\perp} = 2.423$  and  $g_{\parallel} = 2.005$ , which are typical values for the low-spin Co<sup>II</sup> ions ( $S = 1/2$ ). The antiferromagnetic superexchange interaction between Co<sup>II</sup> ions via C<sub>60</sub> is confirmed from the observation of the finite Weiss temperature, which is further supported by the absence of the hyperfine splitting due to <sup>59</sup>Co ( $I = 7/2$ ) nuclei. As the temperature is lowered, the  $g_{\perp}$ -value decreases monotonically suggesting an increase of the crystal-field splitting energy. This result is consistent with the fact that the intermolecular distance between Co<sup>II</sup> and C<sub>60</sub> becomes shorter as the temperature decreases. The peak-to-peak ESR linewidths  $\Delta H_{pp}$  along both principal axes increase with temperature due to the shorter spin–lattice relaxation time.

### 1. Introduction

Because the fullerene C<sub>60</sub> shows a wide variety of physical properties [1–3], many kinds of material which contain C<sub>60</sub> have been synthesized and extensively investigated. In addition, C<sub>60</sub> is also expected to become a uniquely valuable building block in supramolecular construction. On the other hand, it is known that the round shape of C<sub>60</sub> is not appropriate for cocrystallizing with planar molecules and it is necessary to form a concave surface to fit C<sub>60</sub>. Recently, Co, Zn and Fe complexes of octaethylporphyrin (oep) cocrystallite with C<sub>60</sub> have been found to form solids with a remarkably close contact between the curved  $\pi$ -surface of the C<sub>60</sub> with the

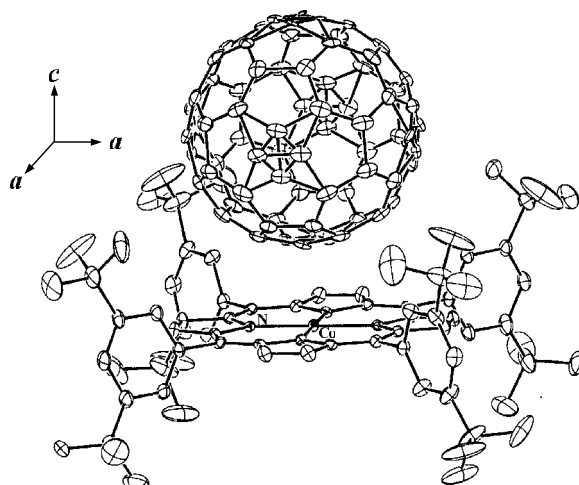


**Figure 1.** A view of the structural unit of  $\text{Co}^{\text{II}}(\text{tbp})\text{-C}_{60}$  determined by room temperature x-ray analysis [8].

planar  $\pi$ -surface of the porphyrin, without the need for matching a convex with a concave surface [4, 5]. In addition, it has been found that the carbon cages of fullerenes are, unusually, not disordered in some of these cocrystallites, due to the intermolecular interaction between fullerene and the metal-(oep) complex [4]. Very recently, such metal-(oep) cocrystallites with  $\text{C}_{60}$  have been extensively synthesized and characterized by using Pd [6], Cu [6], Ag [7] and Ni [7] as the metals of *anti*-formed metal-(oep) complexes.

In this paper we report on the ESR spectra of the newly synthesized  $\text{Co}^{\text{II}}$  complex of 5, 10, 15, 20-tetrakis(3, 5-(di-*tert*-butyl)-phenyl)porphyrin (tbp) cocrystallized with  $\text{C}_{60}$ . In this material, three significant characters of the strong intermolecular interaction between the  $\text{Co}^{\text{II}}(\text{tbp})$  molecule and  $\text{C}_{60}$  have been revealed by x-ray structural analyses [8]. Firstly, it is found that the free rotation of the  $\text{C}_{60}$  molecule is suppressed and thus the absolute positions of the carbon atoms on the  $\text{C}_{60}$  are completely determined even at room temperature. In the cocrystallites with the fullerene containing the most porphyrin, it has been necessary to lower the temperature to determine the complete structure to avoid the disorder caused by the rotation of the fullerene molecule. This characteristic feature of  $\text{Co}^{\text{II}}(\text{tbp})\text{-C}_{60}$  is due to the tight three-dimensional packing between  $\text{C}_{60}$  and  $\text{Co}^{\text{II}}$  porphyrin with four di-*tert*-butylphenyl groups (see figure 1). Secondly, a quite short distance has been observed between a  $\text{Co}^{\text{II}}$  ion and a carbon atom on  $\text{C}_{60}$  (2.61 Å at 293 K) and it decreases with temperature (2.58 Å at 83 K). Such close contact makes possible covalent bonding between them. Lastly,  $C_4$  symmetrical disorder of the carbon atoms on  $\text{C}_{60}$  is observed, although each isolated  $\text{C}_{60}$  molecule does not itself possess  $C_4$  symmetry. This unusual  $C_4$  symmetry of  $\text{C}_{60}$  in this material is attributable to the effect of the  $\text{Co}^{\text{II}}(\text{tbp})$  molecule, which has  $C_4$  symmetry.

Since each structural unit of  $\text{Co}^{\text{II}}(\text{tbp})\text{-C}_{60}$  has a magnetic  $\text{Co}^{\text{II}}$  ion, ESR spectroscopy is a powerful tool for clarifying the variation of the intermolecular interaction between  $\text{Co}^{\text{II}}(\text{tbp})$  and  $\text{C}_{60}$ , as well as that between the  $\text{Co}^{\text{II}}(\text{tbp})$  molecules via the bulky  $\text{C}_{60}$  molecules in this system. In view of this, we report herein the temperature dependence of the ESR spectra and discuss the variation of the  $g$ -values and linewidths, as well as the spin susceptibility in this system. Some of the ESR data were briefly presented in our earlier paper, together with the x-ray structural analyses [8].

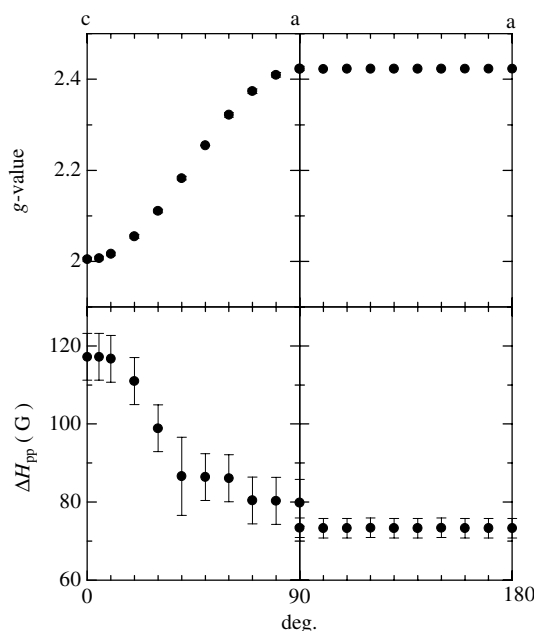


**Figure 2.** The angular dependence of the  $g$ -value and  $\Delta H_{\text{pp}}$  for  $\text{Co}^{\text{II}}(\text{tbp})\cdot\text{C}_{60}$  obtained at room temperature.

## 2. Experimental procedure

The  $\text{Co}^{\text{II}}(\text{tbp})$  molecule has been synthesized by modifying the terminal phenyl ligand of tetraphenylporphyrin (tpp) into di-*tert*-butylphenyl groups. The single-crystalline sample of  $\text{Co}^{\text{II}}(\text{tbp})\cdot\text{C}_{60}$  has been synthesized by the evaporation of a mixture of a solution of the fullerene in toluene and a solution of the  $\text{Co}^{\text{II}}(\text{tbp})$  in toluene as described elsewhere [8]. ESR measurements were performed by using a Bruker E500 X-band spectrometer equipped with a gas-flow-type cryostat, Oxford ESR-900. Sample temperature was controlled by an Oxford ITC 601. The absolute magnitude of the spin susceptibility and  $g$ -value were calibrated using  $\text{CuSO}_4\cdot 5\text{H}_2\text{O}$  and diphenylpicrylhydrazyl (DPPH) as the standard, respectively. The single-crystalline sample was mounted on a Teflon sample holder using normal silicon grease.

## 3. Experimental results and discussion

Figure 1 shows a view of the structural unit of  $\text{Co}^{\text{II}}(\text{tbp})\cdot\text{C}_{60}$  determined at room temperature. This complex crystallizes in the tetragonal space group  $I$  (no 79), with cell dimensions at room temperature of  $a = 20.399(2)$  Å,  $c = 12.0635(8)$  Å and  $V = 5020.1(6)$  Å<sup>3</sup>. The detailed crystal data and three-dimensional packing of  $\text{Co}^{\text{II}}(\text{tbp})\cdot\text{C}_{60}$  are presented in table 1, figure 3 and figure 4 in [8]. The  $\text{Co}^{\text{II}}(\text{tbp})$  is positioned symmetrically between two fullerene units along the  $c$ -direction and the closest contact between the fullerene and the atoms of the  $\text{Co}^{\text{II}}(\text{tbp})$  is achieved in this direction (2.61 Å at room temperature). The fullerene is 'caught' by two porphyrin planes, from top and bottom in the  $c$ -direction, and, further, surrounded by four porphyrins placed side by side in the  $aa$ -plane. The fullerene is located in the position of closest approach to the centred cobalt ion, which involves an electron-rich  $\pi$ -bonding 6:6 carbon ring junction (hexagon–hexagon junction).

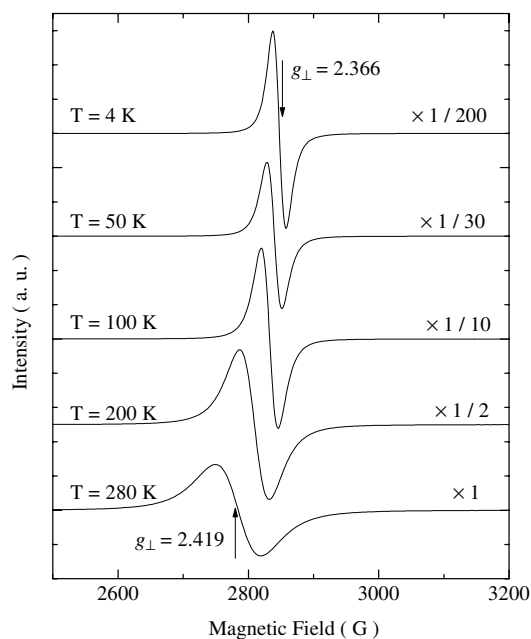


**Figure 3.** Temperature variation of the first-derivative ESR spectra with the magnetic field  $H$  within the  $aa$ -plane. The  $g$ -values are determined from the zero-intensity field represented by the arrows.

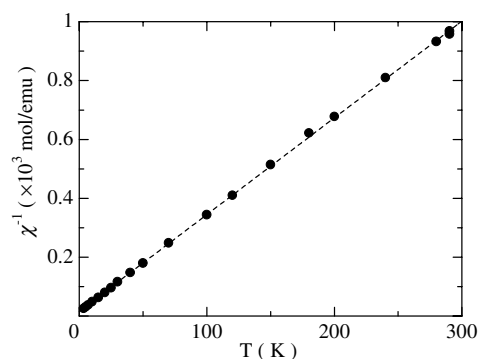


**Figure 4.** Temperature dependence of the inverse spin susceptibility  $\chi^{-1}$  of  $\text{Co}^{\text{II}}(\text{tbp})\text{-C}_{60}$  with the magnetic field  $H$  within the  $aa$ -plane. The dashed line represents the fitting by the Curie–Weiss law.

The magnetic  $\text{Co}^{\text{II}}$  ion is placed in the tetragonal crystal field consisting of four-coordinated nitrogen atoms of the porphyrin molecule and the carbon atoms of the fullerenes. Figure 2 shows the angular dependence of the  $g$ -value and peak-to-peak ESR linewidth  $\Delta H_{\text{pp}}$  of  $\text{Co}^{\text{II}}(\text{tbp})\text{-C}_{60}$  with the external magnetic field  $H$  within the  $ac$ - and  $aa$ -planes at room temperature. Both the  $g$ -values and  $\Delta H_{\text{pp}}$  show uniaxial anisotropy reflected in the tetragonal symmetry of the crystal field, i.e., a large variation in the  $ac$ -plane but almost no change in the  $aa$ -plane. The principal  $g$ -values are obtained as  $g_{\perp}(H \parallel aa\text{-plane}) = 2.423$  and  $g_{\parallel}(H \parallel c\text{-axis}) = 2.005$  at room temperature. These values are typical for the low-spin  $\text{Co}^{\text{II}}$  ions where the unpaired electron resides on the  $\text{Co}(3d_{z^2})$  orbital. In fact, crystal-field theory predicts the following relation for this electron ground state [9]:

$$g_{\perp} = g_e - 6\left(\frac{\zeta}{\Delta E}\right), \quad g_{\parallel} = g_e, \quad (1)$$

where  $g_e$ ,  $\zeta$  and  $\Delta E$  represent the free-electron  $g$ -value (2.0023), the spin-orbit coupling constant ( $\zeta < 0$  for the  $d^7$  configuration) and the energy of the crystal-field splitting between  $d_{z^2}$  and  $d_{x^2-y^2}$ ,  $d_{yz}$  orbitals, respectively. This equation clearly explains the observed anisotropy of the  $g$ -values. Here, we should note that the  $g_{\parallel}$ -value obtained is slightly larger than the theoretical expectation. This discrepancy is often observed for square-planar Co<sup>II</sup> complexes and is attributable to the small mixing of the  $d_{x^2-y^2}$  orbital into the ground-state  $d_{z^2}$  orbital [10].

Figure 3 shows the temperature dependence of the ESR spectra for  $\mathbf{H}$  within the  $aa$ -plane, together with the definition of the  $g$ -value. A nearly Lorentzian-shaped ESR absorption line is observed for the whole temperature region at every direction of  $\mathbf{H}$  and no hyperfine splittings were resolved due to the <sup>59</sup>Co nuclei (natural abundance of 100%,  $I = 7/2$ ). This indicates that hyperfine splitting in this material is averaged out due to the exchange interaction between Co<sup>II</sup> ions, as discussed later. Furthermore, no ESR lines were observed around  $g \sim 1.999$ , which correspond to the absorption by the C<sub>60</sub><sup>-</sup> radical [11]. This indicates that no charge transfers between molecules have occurred in this material, such as [Co<sup>II</sup>(tbp) + C<sub>60</sub> → Co<sup>III</sup>(tbp) + C<sub>60</sub><sup>-</sup>].

Figure 4 shows the temperature dependence of the inverse spin susceptibility  $\chi^{-1}$  for  $\mathbf{H}$  within the  $aa$ -plane. The dashed line represents the fitting by the Curie-Weiss law. The spin susceptibility along the  $c$ -axis showed almost the same tendency as that along the  $aa$ -plane. As can be seen in this figure,  $\chi$  follows the Curie-Weiss law,  $\chi = C/(T + \theta)$ , with the finite antiferromagnetic Weiss temperature  $\theta$ . The estimated value of  $\theta$  is about 4.9 K. The non-zero value of  $\theta$  suggests that there is a finite superexchange interaction between Co<sup>II</sup> ions via the C<sub>60</sub> molecule along the  $c$ -axis, although the Co<sup>II</sup>-Co<sup>II</sup> distance itself is rather large: 12.0635(8) Å at room temperature. This result reflects the close packing between the Co<sup>II</sup>(tbp) and C<sub>60</sub> molecules in this direction, i.e., the wavefunctions of the  $d_{z^2}$  orbital of the Co<sup>II</sup> ion and the curved  $\pi$ -orbital of the fullerene overlap considerably with each other.

To obtain the temperature variation of the intermolecular interaction between the Co<sup>II</sup>(tbp) and C<sub>60</sub>, we plot the principal  $g$ -values of Co<sup>II</sup>(tbp)-C<sub>60</sub> in figures 5(a) ( $g_{\perp}$ ) and (b) ( $g_{\parallel}$ ). Since the wavefunction of the Co(3 $d_{z^2}$ ) orbital, on which the unpaired electron resides, is considered to be sensitive to the location of the C<sub>60</sub> molecules along the  $c$ -direction, these parameters act as sensitive probes of the intermolecular interaction in this material. As shown in figure 5(a), the characteristic behaviour of the  $g_{\perp}$ -value is revealed, i.e., it decreases monotonically with temperature, whereas the  $g_{\parallel}$ -value in figure 5(b) is almost unchanged. This decreasing  $g_{\perp}$ -value directly indicates that the intermolecular interaction increases in the low-temperature region as discussed below. As shown in equation (1), the  $g_{\perp}$ -value shifts by  $6(\zeta/\Delta E)$  from  $g_e$ . Thus the observed decrease of the  $g_{\perp}$ -value indicates the increase of the energy separation  $\Delta E$  at low temperature. In other words, the Co(3 $d_{z^2}$ ) orbital is destabilized as the temperature is lowered. Such behaviour is expected in the case where the intermolecular distance between Co<sup>II</sup>(tbp) and C<sub>60</sub> along the  $c$ -direction is decreasing with temperature. This result agrees excellently with the results of the x-ray structural analyses, which suggest that the interatomic distance between the Co<sup>II</sup> ion and the carbon atom on C<sub>60</sub> decreases from 2.61 Å at 293 K to 2.58 Å at 83 K along the  $c$ -direction [8]. Figure 5(a) further suggests that even shorter contacts should be achieved between the molecules at temperatures below 83 K. On the other hand, equation (1) predicts constant  $g_{\parallel}$ -values of  $g_e$ —which is actually observed, as shown in figure 5(b)—although the value increases slightly in the low-temperature region of  $T < 30$  K. As already mentioned, the  $g_{\parallel}$ -value deviates from  $g_e$  due to the contribution of the Co(3 $d_{x^2-y^2}$ ) orbital. Thus the observed increase of the  $g_{\parallel}$ -value is attributable to the increasing contribution of this orbital. This interpretation is seen to be reasonable if one considers the destabilization

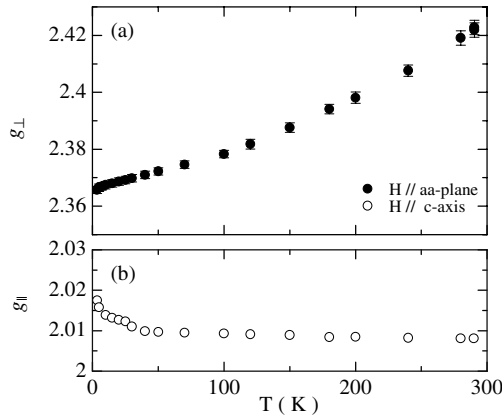


**Figure 5.** Temperature dependences of the principal  $g$ -values: (a)  $g_{\perp}$  and (b)  $g_{\parallel}$ .

of the  $\text{Co}(3d_{z^2})$  orbital in the low-temperature region as discussed above, because it reduces the energy separation between the  $\text{Co}(3d_{x^2-y^2})$  and  $\text{Co}(3d_{z^2})$  orbitals, which may promote the mixing of these two orbitals.

As already mentioned,  $\Delta H_{\text{pp}}$  also shows clear anisotropy in the  $ac$ -plane and this type of anisotropy is observed over the whole temperature region as shown in figure 6, where open and closed circles represent  $\mathbf{H}$  parallel to the  $c$ -axis and within the  $aa$ -plane, respectively. As mentioned before, the temperature dependence of the spin susceptibility  $\chi$  suggests that there is a finite antiferromagnetic superexchange interaction of  $J \simeq 4.9$  K between  $\text{Co}^{\text{II}}$  ions, which is estimated from  $\theta \simeq 4.9$  K for number of nearest-neighbour  $\text{Co}^{\text{II}}$  ions  $Z = 2$  and  $S = 1/2$ . As a result, the eight hyperfine splitting lines of the ESR spectra due to  $^{59}\text{Co}$  nuclei ( $I = 7/2$ ) are averaged out into a single amalgamated line (exchange narrowing). In this case, it is natural to consider the exchange-narrowed hyperfine splitting as the origin of the observed  $\Delta H_{\text{pp}}$ . Then  $\Delta H_{\text{pp}}$  contains the remaining information on the anisotropy and amplitude of the original hyperfine interaction, although the estimation of the hyperfine splitting energy itself is difficult and there remains some ambiguity. For estimating the exchange-narrowed linewidth, Anderson and Weiss have presented the following expression [12]:

$$\Delta H = [(10/3)H_p^2 + H_H^2]/H_e, \quad (2)$$

where  $\Delta H$  represents the half-width at half-power,  $H_p$ ,  $H_H$  and  $H_e$  represent the internal magnetic field due to dipole, hyperfine and exchange interactions, respectively. The first term of equation (2) is negligible due both to the large separation between  $\text{Co}^{\text{II}}$  ions and to the relatively large value of  $H_e$ . In fact, the lattice parameter and observed  $H_e$  lead to a prediction of at most 0.04 G for the dipole interaction term of equation (2) at room temperature, which is three orders of magnitude smaller than the experimental value of  $\Delta H_{\text{pp}}$ . Then on replacing  $H_H$  with  $7|A|$ , the largest splitting of the ESR line between  $m_I = \pm 7/2$  transitions, equation (2) reduces to the following form:

$$\Delta H = 49A^2/H_e, \quad (3)$$

where  $|A|$  represents the hyperfine splitting constant. In the low-spin  $d^7$  electron configuration with the unpaired electron residing on the  $d_{z^2}$  orbital, crystal-field calculation provides the following relations for the principal  $|A|$ -values [9, 13, 14]:

$$A_{\perp} = -P[\kappa + 2/7 - (15/14)(\Delta g_{\perp})] \quad (4)$$

$$A_{\parallel} = -P[\kappa - 4/7 + (1/7)(\Delta g_{\perp})], \quad (5)$$

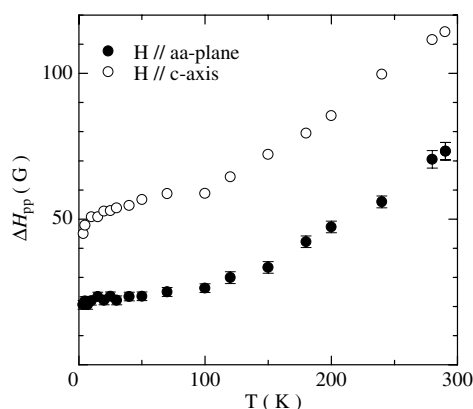


**Figure 6.** Temperature dependences of the ESR linewidth  $\Delta H_{pp}$  with  $H$  parallel to the  $c$ -axis (open circles) and within the  $aa$ -plane (solid circles).

where  $\kappa$  is the isotropic Fermi contact term and  $P = g_e g_N \beta_e \beta_N < 3 d_{z^2} |r^{-3}| 3d_{z^2} >$  ( $=0.022 \text{ cm}^{-1}$  for free  $\text{Co}^{\text{II}}$  ions [15]).  $\Delta g_{\perp}$  represents the shift of  $g_{\perp}$ -value from  $g_e$  which is given in equation (1). Using these equations, we discuss the observed behaviours of  $\Delta H_{pp}$  in this material. As shown in figure 6,  $\Delta H_{pp}$  along the  $c$ -axis is larger than  $\Delta H_{pp}$  along the  $a$ -axis over the whole temperature region. As predicted from equation (5), this is attributable to the anisotropy of  $|A|$ , i.e.,  $|A_{\parallel}| > |A_{\perp}|$ . This type of anisotropy is often seen in the low-spin  $\text{Co}^{\text{II}}$  complexes [14, 16, 17]. In addition, figure 2 further suggests that the  $g$ - and  $A$ -tensors of this material have the same principal axes because the extremal values of  $g$  and  $\Delta H_{pp}$  are observed at the same angles within experimental error. We mention here the order estimation for the  $|A|$ -values, fixing  $H_e$  to the experimentally obtained  $J$  of 4.9 K ( $\simeq 30\,000$  G). At  $T = 70$  K, equation (3) predicts  $|A_{\perp}| \simeq 125$  G and  $|A_{\parallel}| \simeq 190$  G. These values are comparable to the typical value of 170 G, which is given by Yudanov *et al* for the analogous complexes  $\text{Co}(\text{tpp})\cdot\text{C}_{60}(\text{CS}_2)_{0.5}$  and  $\text{Co}(\text{tpp})\cdot\text{C}_{70}$  [18, 19].

On the other hand,  $\Delta H_{pp}$  shows remarkable broadening along both axes especially in the high-temperature region as shown in figure 6. There are two possibilities for explaining this temperature dependence of  $\Delta H_{pp}$ , i.e., the temperature variation of the  $|A|$ -values due to the shift of the  $g_{\perp}$ -value and the dominance of the spin–lattice relaxation time  $T_1$  at higher temperatures. The former possibility is, however, excluded by the following consideration. Since the third terms of equation (5) for both principal axes are proportional to the temperature-dependent value of  $\Delta g_{\perp}$  which is shown in figure 5(a), the  $|A|$ -values can be modified as the temperature increases. But in such a case, equation (5) allows the  $|A|$ -value to increase with temperature only for one principal axis and not for both axes. For example, if we adopt the experimentally obtained  $\Delta g_{\perp}$  values for this material and  $\kappa \simeq 0$ , which is observed for the  $\text{Co}^{\text{II}}$  phthalocyanine complex [13], equation (5) shows that  $|A_{\perp}|$  will increase with the  $\Delta g_{\perp}$  value, but  $|A_{\parallel}|$  will, in contrast, decrease as the temperature increases. Furthermore, no matter how the value of  $\kappa$  is adjusted, equation (5) is incapable of explaining the observed behaviour of  $\Delta H_{pp}$ . Thus it is concluded that the smaller value of  $T_1$  at higher temperatures should be the main origin of the observed broadening of  $\Delta H_{pp}$ . It is reported that the square-planar  $\text{Co}^{\text{II}}(\text{tpp})$  complex exhibits no ESR spectra at room temperature due to a small  $T_1$ -value [19, 20]. This may be consistent with the observation of line broadening for the current material. It should be noted that the dominance of the spin–lattice relaxation time in the high-temperature region would not change the estimation of  $|A|$ -values at 70 K discussed above because it is expected that  $T_1$  will become larger rapidly with decreasing temperature [21].



On the basis of the ESR measurements above, the electronic ground state of Co(tbp)-C<sub>60</sub> has become clear and the features of the temperature-dependent intermolecular interaction between Co(tbp) and C<sub>60</sub> are clarified. As the next step, photoinduced changes of ESR spectra may provide information on the charge transfer from Co(tbp) to fullerene. Such measurements are now under way.

#### 4. Conclusions

We made ESR measurements on the newly synthesized cocrystallite of C<sub>60</sub> with the Co<sup>II</sup>(tbp) complex. Both the spin susceptibility  $\chi$  and the absence of <sup>59</sup>Co hyperfine structure suggest the existence of a superexchange interaction between Co<sup>II</sup> ions via the C<sub>60</sub> molecule in this material. We found temperature-dependent *g*-values, this dependence arising from the increase in crystal-field splitting energy of the Co(3d) orbitals, providing evidence of the increase in intermolecular interaction as the temperature is lowered. This result is consistent with the x-ray structural analyses which show that the intermolecular distance between Co<sup>II</sup>(tbp) and C<sub>60</sub> decreases with temperature. In addition, temperature-dependent ESR linewidths are observed along both axis, which may be attributable to the shorter spin–lattice relaxation time in the high-temperature region.

#### Acknowledgment

This work was partially supported by a Grant-in-Aid for Scientific Research from the Ministry of Education, Culture, Sports, Science and Technology of Japan.

#### References

- [1] Kroto H W, Heath J R, O'Brien S C, Curl R F and Smalley R E 1985 *Nature* **318** 162
- [2] Hebard A F, Rosseinski M J, Haddon R C, Murphy D W, Glarum S H, Palstra T T M, Ramirez A P and Kortan A R 1991 *Nature* **350** 600
- [3] Allemand P M, Khemani K C, Koch A, Wudl F, Holczer K, Donovan S, Gruner G and Thompson J D 1991 *Science* **253** 301
- [4] Olmstead M M, Costa D A, Maitra K, Noll B C, Phillips S L, Van Calcar P M and Balch A L 1999 *J. Am. Chem. Soc.* **121** 7090
- [5] Hochmuth D H, Michel S L J, White A J P, Williams D J, Ballet A G M and Hoffman B M 2000 *Eur. J. Inorg. Chem.* 593
- [6] Ishii T, Aizawa N, Yamashita M, Matsuzaka H, Kodama T, Kikuchi K, Ikemoto I and Iwasa Y 2000 *J. Chem. Soc. Dalton Trans.* **23** 4407
- [7] Ishii T, Aizawa N, Kanehama R, Yamashita M, Matsuzaka H, Kodama T, Kikuchi K and Ikemoto I 2001 *Inorg. Chim. Acta* **317** 81
- [8] Ishii T, Kanehama R, Aizawa N, Yamashita M, Matsuzaka H, Sugiura K, Miyasaka H, Kodama T, Kikuchi K, Ikemoto I, Tanaka H, Marumoto K and Kuroda S 2001 *J. Chem. Soc. Dalton Trans.* 2975
- [9] Maki A H, Edelstein N, Davison A and Holm R H 1964 *J. Am. Chem. Soc.* **86** 4580
- [10] Nowlin T, Subramanian S and Cohn K 1972 *Inorg. Chem.* **11** 2907
- [11] Allemand P-M, Srdanov G, Koch A, Khemani K and Wudl F 1991 *J. Am. Chem. Soc.* **113** 2781
- [12] Anderson P W and Weiss P R 1953 *Rev. Mod. Phys.* **25** 269
- [13] Griffith J S 1958 *Discuss. Faraday Soc.* **26** 81
- [14] Wayland B B, Minkiewicz J V and Abd-Elmageed M E 1974 *J. Am. Chem. Soc.* **96** 2795
- [15] Abragam A and Pryce M H L 1951 *Proc. R. Soc.* **206** 173
- [16] Walker F A 1970 *J. Am. Chem. Soc.* **92** 4235
- [17] Symons M C R and Wilkinson J G 1971 *J. Chem. Soc. A* 2069
- [18] Konarev D V, Yudanova E I, Neretin I S, Slovokhotov Yu L and Lyubovskaya R N 2001 *Synth. Met.* **121** 1125
- [19] Yudanova E I, Konarev D V, Gumanov L L and Lyubovskaya R N 1999 *Russ. Chem. Bull.* **48** 718
- [20] Assour J M 1965 *J. Chem. Phys.* **43** 2477
- [21] Orton J W 1968 *Electron Paramagnetic Resonance* (London: Iliffe) ch 9